THE JOURNAL OF PHYSICAL CHEMISTRY LETTERS
A JOURNAL OF THE AMERICAN CHEMICAL SOCIETY

pubs.acs.org/JPCL Letter

# Spatiotemporal Control of Ice Crystallization in Supercooled Water via an Ultrashort Laser Impulse

Hozumi Takahashi, Tatsuya Kono, Kosuke Sawada, Satoru Kumano, Yuka Tsuri, Mihoko Maruyama, Masashi Yoshimura, Daisuke Takahashi, Yukio Kawamura, Matsuo Uemura, Seiichiro Nakabayashi, Yusuke Mori, Yoichiroh Hosokawa,* and Hiroshi Y. Yoshikawa*

Cite This: *J. Phys. Chem. Lett.* 2023, 14, 4394−4402 Read Online

ACCESS | Metrics & More | Article Recommendations | Supporting Information

**ABSTRACT:** Focused irradiation with ultrashort laser pulses realized the fine spatiotemporal control of ice crystallization in supercooled water. An effective multiphoton excitation at the laser focus generated shockwaves and bubbles, which acted as an impulse for inducing ice crystal nucleation. The impulse that was localized close to the laser focus and accompanied by a small temperature elevation allowed the precise position control of ice crystallization and its observation with spatiotemporal resolution of micrometers and microseconds using a microscope. To verify the versatility of this laser method, we also applied it using various aqueous systems (e.g., plant extracts). The systematic study of crystallization probability revealed that laser-induced cavitation bubbles play a crucial role in inducing ice crystal nucleation. This method can be used as a tool for studying ice crystallization dynamics in various natural and biological phenomena.

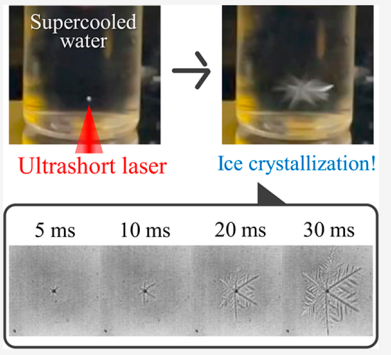




Ice crystallization plays a crucial role in various natural and biological phenomena and thus has attracted much attention in many scientific and industrial fields. For instance, ice crystals, including "snow", show a wide variety of morphologies depending on environmental parameters, such as temperature and pressure, so their morphological diagrams and growth conditions have been intensively studied in glaciology, cloud physics, and pattern formation science.[1−3] Ice crystallization in the presence of biological materials, such as saccharides and antifreeze proteins (AFPs), has also been considered in cryobiology to elucidate the freezing tolerance mechanisms of organisms and plants inhabiting subfreezing environments.[4−6] This knowledge also provides key insights into the development of food processing methods.[7]

To reveal the ice crystallization mechanisms, the precise measurement of ice crystal growth was performed by using a crystal seed, which was prepared in advance, for example, by transporting a seed into a crystal growth cell from a capillary.[8−12] However, it is not trivial to precisely monitor the spatiotemporal dynamics of an early stage of ice crystallization, including nucleation in bulk water, which starts stochastically and proceeds very rapidly. Indeed, experimentally investigating ice crystal nucleation using optical microscopy is considerably challenging because of the contingency of nucleation. To observe such a stochastic and transient event, a number of studies have proposed using seedless methods to trigger ice crystallization by external stimuli. One of the major methods is a sudden drop in temperature (called quenching). However, quenching is not intrinsically suited to controlling ice nucleation in a spatial and temporal manner; hence, its application is limited to tiny water droplets at extremely low temperatures (e.g., several microliters and minus tens of degrees Celsius)[13−15] because of limited camera fields-of-view and very short exposure times. Alternatively, external stimuli, such as electric effects,[16] ultrasound,[17] lasers,[18,19] etc., have been proposed as a means of spatiotemporally controlling ice nucleation.

Among these methods, impulse induced by laser pulses is promising for studies of ice crystals growing in bulk water at very low temperatures (e.g., ≪−10 °C) and the early stage of ice crystallization (e.g., nucleation) using optical microscopy. When intensive laser pulses are focused into the liquid through an objective lens, pressure waves and transient vapor/gas bubbles (cavitation bubbles)[20−22] are generated in nanoseconds to microseconds, which can act as the impulse to trigger crystal nucleation.[23] Compared to the use of unfocused pulsed lasers, which triggers nucleation along the pathway of the laser via photoelectric fields,[19,24] the impulse that is generated by the focused irradiation with ultrashort laser pulses could exhibit higher spatial controllability of nucleation. Actually, several studies have demonstrated the precise control of crystal nucleation of various compounds such as proteins

**Received:** February 14, 2023
**Accepted:** April 7, 2023
**Published:** May 8, 2023

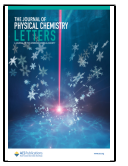





https://doi.org/10.1021/acs.jpclett.3c00414
*J. Phys. Chem. Lett.* 2023, 14, 4394−4402

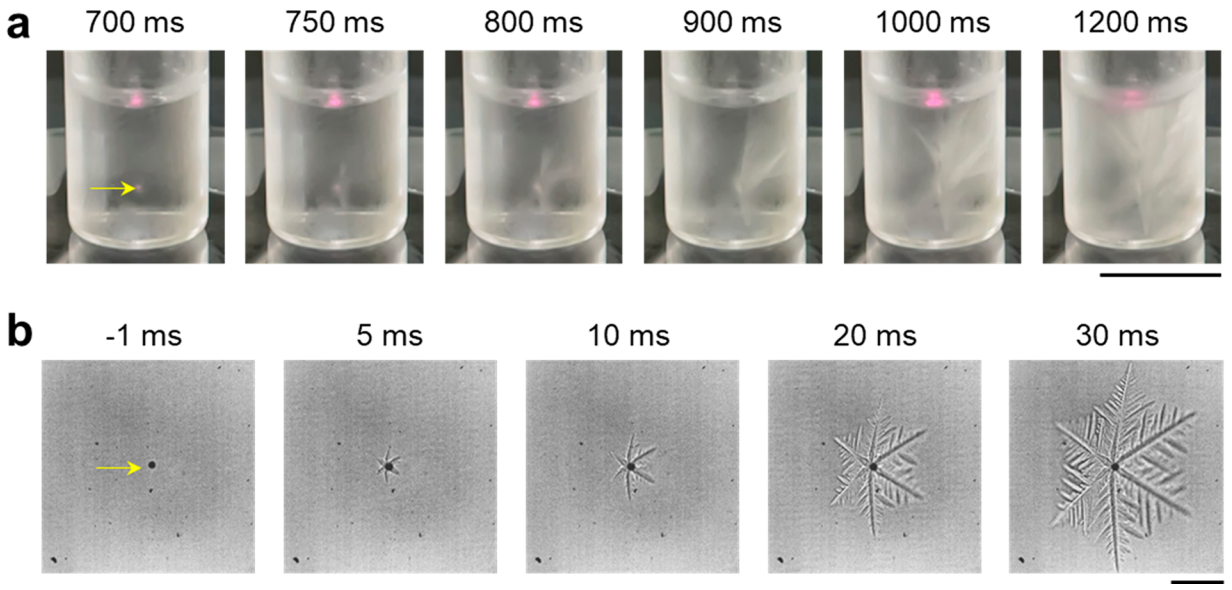


**Figure 1.** Ice crystallization via laser irradiation. (a) Macroscopic and (b) microscopic images of ice crystallization behavior triggered by laser pulses [(a) $E$ = 10 $\mu$J/pulse, $\Delta t$ = 250 fs, 20 Hz, $T \approx -5$ °C; (b) $E$ = 3 $\mu$J/pulse, $\Delta t$ = 150 fs, 20 Hz, $T = -5$ °C]. The yellow arrow indicates the focal spot. $t$ = 0 ms is defined as (a) the time when the laser irradiation started and (b) the time of the laser irradiation that subsequently generated the ice crystal. The scale bars represent (a) 10 mm and (b) 200 $\mu$m. The images were captured at frame rates of (a) ~240 fps and (b) 10000 fps.

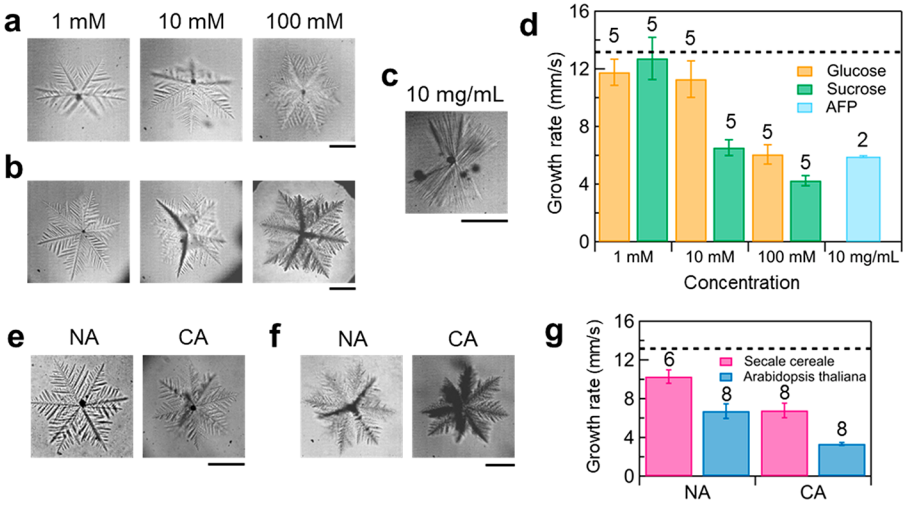


**Figure 2.** Ice crystals produced under various conditions. Ice crystals generated in (a) glucose, (b) sucrose, and (c) antifreeze protein (AFP) solution by laser irradiation ($E \approx 3$ $\mu$J/pulse, $\Delta t$ = 150 fs, (a and b) 20 Hz, (c) 1 kHz, $T = -5.0$ °C). According to the previous studies,[27,28] freezing temperature of saccharide solution and AFP solution were estimated to be approximately −5 to −4.8 °C and ~−4 °C, respectively. (d) Dependence of the additive concentration on the growth rate. Ice crystals generated in extract solution from (e) *Secale cereale* and (f) *Arabidopsis thaliana* by laser irradiation ($E \approx 3$ $\mu$J/pulse, $\Delta t$ = 150 fs, 20 Hz, $T = -5.0$ °C). NA, nonacclimated plant; CA, cold-acclimated plant. (g) Dependence of the culture conditions on the growth rate. The growth rate was measured for the first 50 ms after laser irradiation, which triggered crystal nucleation. The black dashed line shown in panels d and g corresponds to the growth rate of ice in pure water. The sample numbers tested are shown for each condition. The images were captured at frame rates of 10000 fps. The scale bars represent 200 $\mu$m. Some of the ice crystal images were reproduced with modification from the literature.[29]

and organic compounds by utilizing the laser-induced impulses.[23] Regarding the application of laser-induced impulses in ice crystallization, in 2007, Lindinger et al. demonstrated ice crystallization with focused nanosecond laser pulses with a wavelength of 1064 nm.[18] However, due to the relatively low spatiotemporal controllability and thermal disturbance of impulses generated by nanosecond laser irradiation at 1064 nm, detailed dynamics, such as the morphological development of ice crystals from a focal point, are still unclear. To gain further insights into ice crystallization with higher spatiotemporal resolution, it is necessary to utilize laser pulses with much shorter pulse durations, which can act as a fine-tuned, thermal-less trigger for controlling the crystallization of various materials.[23]

In this work, we have demonstrated the fine-tuned, spatiotemporal control of ice crystal nucleation and crystal growth in supercooled water via focused irradiation of ultrashort laser pulses (picosecond and femtosecond pulses) with the wavelength of smaller optical absorption by water (i.e., $\lambda$ = 800 nm), which can induce well-localized impulses due to the generation of cavitation bubbles and shockwaves with small heat effects at the laser focus in liquids via effective



https://doi.org/10.1021/acs.jpclett.3c00414
J. Phys. Chem. Lett. 2023, 14, 4394−4402

multiphoton excitation. This method could realize the high-speed microscopic imaging of ice crystallization dynamics with resolutions of micrometers and microseconds. We also demonstrated the fine control of ice crystallization in various aqueous solutions, such as glucose, sucrose, AFP, and plant extract solutions. With a sequential pulse irradiation with a repetition rate of 1 kHz, we observed a stepwise crystal growth that followed each laser irradiation.

Figure 1a shows macroscopic images of ice crystallization in a glass vial induced by femtosecond laser pulses ($T \approx -5$ °C, see also Movie S1). After the onset of laser irradiation, ice crystals were formed from the laser focus ($t \approx 700$ ms) and immediately filled the entire glass vial. To obtain further insights into the dynamics of laser-induced ice crystallization, we used an optical microscope combined with a femtosecond (picosecond) laser amplification system. Figure 1b shows microscopic images of ice crystallization induced with femtosecond laser pulses ($T = -5$ °C, see also Movie S2). The black circle shadow observed at the center of the picture at $t = -1$ ms corresponds to a bubble that was generated by prelaser irradiation (in this case, ~10 times laser irradiation). The bubbles can mainly be attributed to dissolved gas and/or chemical products from water (denoted as long-lasting bubbles).[25,26] By repeatedly irradiating with laser pulses, a single dendritic ice crystal suddenly appeared next to the bubbles ($t = 0$ ms). The growth rate of the tip of the ice crystal was 1.3 cm/s on average, which is almost on the same order as the previously reported value without laser irradiation (~1 cm/s)[3]. It should be noted that the location of ice crystal generation was within 63 ± 32 μm ($n = 26$) from the laser focus, indicating that the spatial controllability of ice crystallization with a femtosecond laser is better than that reported in a previous study with a nanosecond laser (~300 μm).[18]

Studies of ice crystallization in the presence of biomolecules are crucially important for elucidating the underlying freezing tolerance mechanisms of animals, plants, and organisms. To verify the versatility of this laser method for such studies of ice crystallization with additional components, we then tested the laser-induced crystallization of several aqueous solutions (pure water, glucose, sucrose, AFP, and plant extract solutions). Figure 2a–c shows ice crystals that were produced in glucose solution, sucrose solution, and AFP solution with femtosecond laser pulses ($T = -5$ °C, see also Movies S3, S4, and S5), respectively. Ice crystals grown in the presence of glucose and sucrose (Figure 2a,b) showed more branches than those grown in pure water (Figure 1b). In addition, the number of crystal branches increased with increasing saccharide concentration. On the other hand, ice crystals in the presence of AFP became needle-like in shape (Figure 2c). Figure 2d shows the dependence of the additive concentration on the crystal growth rate. The growth rate of ice crystals grown with additives was smaller than that of ice crystals grown with pure water and tended to decrease with increasing additive concentration. The tendency of crystal morphology and growth rate of ice crystals grown with laser irradiation were consistent with those grown without laser irradiation.[28,30]

Moreover, as a complex system, we demonstrated ice crystallization from extract solutions of *Secale cereale* and *Arabidopsis thaliana* with cold acclimation ($T = -5$ °C, Figure 2e,f, see also Movies S6 and S7). The morphology of the laser-induced ice crystals was dendritic with many branches. The growth rate of these crystals (Figure 2g) was lower than that of ice crystals grown in pure water. Additionally, the crystal growth was significantly decreased in solutions extracted from plants with cold acclimation that were kept at low temperatures for several days. These results clearly indicate that the laser-induced impulse enables us to precisely monitor the dynamics of ice crystallization with various additives including biological samples, providing important insights into ice-related scientific fields, such as cryobiology.

To optimize the spatiotemporal controllability of laser-induced ice crystallization, we then explored pulse duration and pulse energy dependences to induce ice crystallization with fewer laser pulses. We found that irradiation with a pulse duration of 5 ps could effectively induce ice crystallization even with a single pulse ($T \approx -10$ °C, Figure 3a, see also Movie S8). The probability of ice crystal nucleation with a single laser pulse is summarized in Figure 3b. In the 150 fs pulse case, focused irradiation rarely induced ice crystallization even with the systematic screening of laser energy (<4% at $E = 60$ μJ/pulse, 0.9% calculated from 1 nucleation for 111 attempts for the entire energy range $E = 10$–240 μJ/pulse). On the other hand, in the cases of 1, 5, and 100 ps pulse irradiation, a higher probability of ice crystallization was obtained above certain laser energy thresholds (1 ps: ≥180 μJ/pulse; 5 ps: ≥60 μJ/pulse; 100 ps: ≥120 μJ/pulse), indicating that a certain magnitude of laser-induced impulse is necessary for the induction of ice crystal nucleation. Their crystallization probabilities increased with increasing laser energy (1 ps: 5% → 30%; 5 ps: 20% → 80% → 100%; 100 ps: 5% → 15% → 65%). Figure S1 shows the dependence of the laser energy on the crystal nucleation probability using 10 ns pulses. Crystal nucleation was induced at $E \geq 1000$ μJ/pulse. The probability saturated at approximately 60% with $E \geq 1400$ μJ/pulse. Our recent work demonstrated crystal nucleation from glacial acetic acid melt by focused laser pulses and revealed that larger cavitation bubbles resulted in a higher crystal nucleation probability.[31] In this study of ice crystallization, we also found

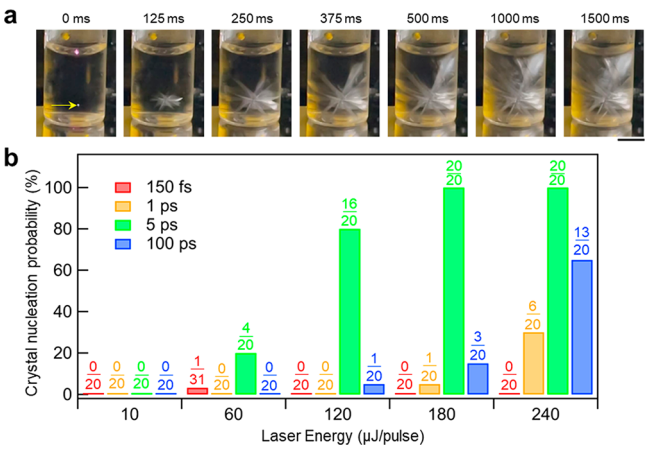


**Figure 3.** Ice crystallization via a single laser pulse. (a) Representative ice crystallization behavior triggered by a single laser shot ($E = 240$ μJ/pulse, $\Delta t = 5$ ps, $T \approx -10$ °C). The images were captured at a frame rate of 240 fps. A single laser pulse was shot at $t = 0$ ms. The yellow arrow indicates the laser focus. The scale bar represents 5 mm. (b) Dependence of the laser energy and pulse duration on the ice crystal nucleation probability. Here, crystal nucleation probability was defined as the ratio of sample numbers nucleated to the total sample numbers. The ratio of the sample number nucleated to the total sample number is shown for each condition.



https://doi.org/10.1021/acs.jpclett.3c00414
J. Phys. Chem. Lett. 2023, 14, 4394–4402

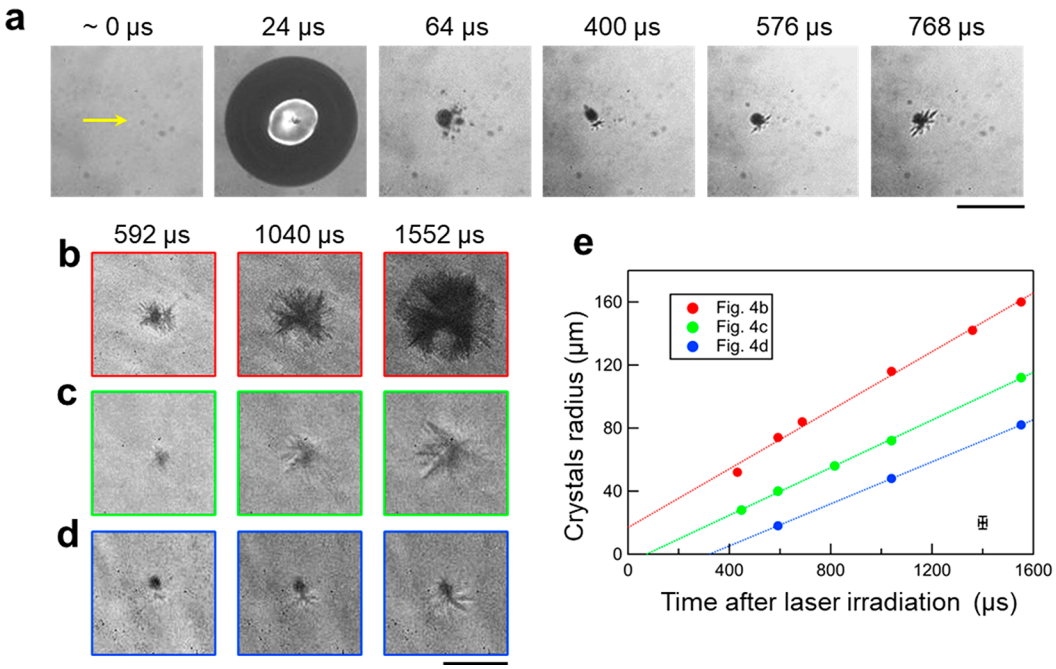


**Figure 4.** High-speed imaging of ice crystallization behavior. (a–d) Representative ice crystal dynamics induced by a single laser pulse ($E$ = 240 $\mu$J/pulse, $\Delta t$ = 5 ps, $T \approx -10$ °C). The images were captured at frame rates of (a) 125000 fps and (b–d) 62500 fps. The yellow arrow indicates the laser focus. The scale bars represent 200 $\mu$m. (e) Temporal change in the ice crystal radius after laser irradiation in Figure 4b–d. The growth rates estimated from the slope of the linear fitting curve are 7–9 cm/s, of which rates are comparable to that of without laser irradiation reported previously.[3] Uncertainties in the bottom right correspond to a single frame exposure time (16 $\mu$s) and ±1 pixel (4 $\mu$m).

that there is such correlation between the crystallization probability (Figure 3b) and maximum cavitation bubble radius (Figure S2). For instance, ice nucleation could be induced by laser irradiation with the energy that can generate the cavitation bubble with a maximum diameter of ~200 $\mu$m. Besides, in the energy regime ($E$ = 60–240 $\mu$J/pulse) and pulse durations (150 fs, 1 ps, 5 ps, and 100 ps), the cavitation bubble with a 5 ps pulse showed the largest bubble size and the highest nucleation probability. Moreover, compared with the nucleation probability in the same laser energy (e.g., $E$ = 180, 240 $\mu$J/pulse), the order of probability tended to follow the order of the size of a cavitation bubble (150 fs < 1 ps < 100 ps < 5 ps). Such pulse duration dependence on cavitation bubble sizes is attributed to various factors such as nonlinear absorption coefficient (almost no one-photon absorption of water at $\lambda$ = 800 nm), heat diffusion, thermoelastic pressure,[32,33] which should significantly influence water vaporization at a laser focus. These results imply that cavitation bubbles play a crucial role in ice crystal nucleation. It should be noted that the crystal nucleation probabilities using a 5 ps pulse were typically higher than when using 150 fs, 1 ps, 100 ps, and 10 ns pulses.

On the basis of the above-mentioned results, we carried out high-speed imaging of ice crystallization dynamics with a single laser pulse at $\Delta t$ = 5 ps. The representative results are shown in Figures 4a and 4b–d, where ice crystallization dynamics were observed at 125000 and 62500 frames per second (fps), respectively ($T \approx -10$ °C, see also Movies S9 and S10). It should be noted that these frame rates are more than 50 times higher than those in the study of nanosecond lasers.[18] Upon laser irradiation ($t$ = 0 $\mu$s), a cavitation bubble was formed at the laser focus. The size reached the maximum radius (~400 $\mu$m) at approximately $t$ = 24 $\mu$s. The cavitation bubble started to shrink and finally collapsed at $t$ = 64 $\mu$s with multiple processes of shrinkage and re-expansion. Afterward, long-lasting bubbles appeared and moved away from the laser focus, which is probably due to the liquid flow induced by collapse of a cavitation bubble. After the flow was gone, the movement of the long-lasting bubbles slowed down. Approximately 400 $\mu$s later, a single ice crystal was observed next to the long-lasting bubbles, as shown in Figure 1b. The ice crystal grew and finally became dendritic in form. Note that ice crystals were typically observed at the long-lasting bubbles but not always (Figure S3). Although the cavitation bubble size for the picosecond pulse at $E$ = 240 $\mu$J/pulse should be larger than that for fs pulses at $E$ = 3 $\mu$J/pulse (Figure 1b), we found that ice crystals were observed at 77 ± 46 $\mu$m ($n$ = 28) from the laser focus typically with long-lasting bubbles, and the spatial resolution of the laser-induced ice crystallization was still higher than that of the nanosecond laser-induced ice crystallization (~300 $\mu$m).[18]

Figure 4e shows the representative time evolution of the ice crystal radius after laser irradiation. The crystal size increased almost linearly over time. The other attempts that we ran to collect the data of Figure 4 (not shown here) were mostly located between the red and blue lines in Figure 4e. If we assume that the intersection between the linear fitting and the bottom axis represents the time of nucleation events, this result indicates that the timing of ice crystal nucleation is not always the same but fluctuates in the range of several hundred microseconds after laser irradiation (Figure 4b–d), implying that several phenomena such as shockwaves, cavitation bubbles, and long-lasting bubbles (this will be discussed later) are involved in the laser-induced nucleation mechanism. It should be noted that, in some events, the intersection between fitting lines and the $x$-axis (time) in Figure 4e becomes negative values (e.g., a red line). This means that there is nonlinearity in the crystal growth; that is, the growth



https://doi.org/10.1021/acs.jpclett.3c00414
J. Phys. Chem. Lett. 2023, 14, 4394–4402

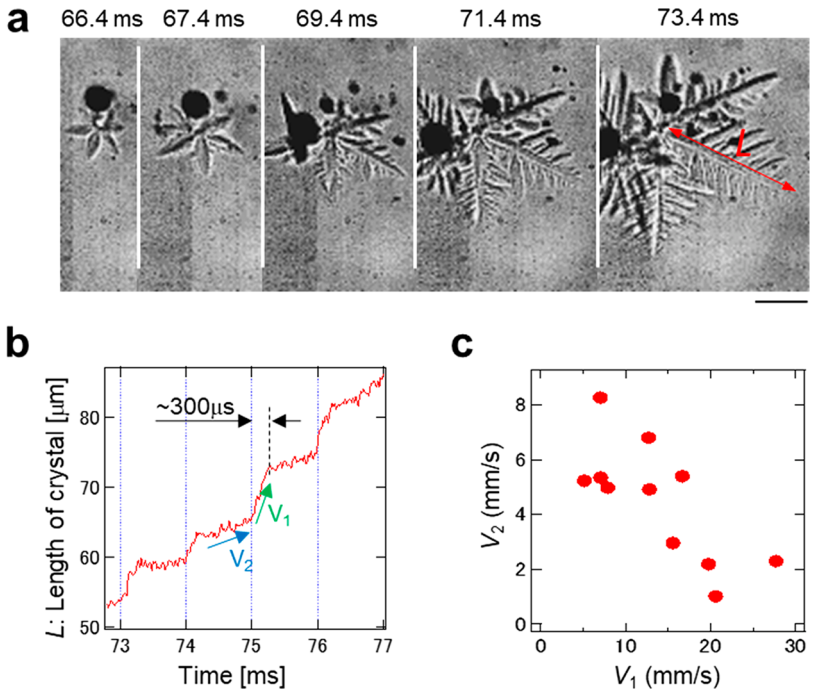


**Figure 5.** Stepwise growth enhancement of ice crystals triggered by laser irradiation. (a) Microscopic image of ice crystallization behavior induced by laser pulses ($E$ = 1.3 $\mu$J/pulse, $\Delta t$ = 250 fs, 1 kHz, $T$ = −5 °C). The elapsed time after the onset of laser irradiation ($t$ = 0 ms) is shown above the photographs. The crystal was observed after 65 ms of irradiation with laser pulses. The scale bar represents 200 $\mu$m. Images were captured at a frame rate of 50000 fps. (b) Temporal change in the crystal length ($L$) in the time regime of 72.8−77.0 ms. Laser pulses are introduced at the timing indicated by the blue dotted lines in the graph. (c) Relationship between $V_1$ and $V_2$ for each shot after crystal growth began.

rate of ice crystals presumably slows down because of accumulation of latent heat.

These results indicate that laser-induced ice crystallization with a single pulse enabled us to observe the crystallization dynamics with an extremely high spatial resolution (~100 $\mu$m) and frame rate (up to 125000 fps), which are superior to those of a previous study.[18] Considering the frame rate (maximum: 1000000 fps) and field-of-view (~1 × 1 mm) of this study, it should be noted that we can monitor the early stage of ice crystal crystallization dynamics at a speed of even 10 m/s and more with micrometer spatial resolution, indicating that this laser method can be a tool for studying ice crystallization dynamics at low temperatures (e.g., ≪−10 °C), which few studies have reported thus far. Such microscopic studies of ice crystal growth under extreme supercooling should elucidate various physical phenomena that occur during the temporal evolution of the dendritic crystal growth morphology.

In addition to crystal nucleation, we observed a unique stepwise crystal growth behavior that followed each laser irradiation. Figure 5a shows the microscopic ice crystallization dynamics triggered by laser irradiation with a repetition rate of 1 kHz ($E$ = 1.2 $\mu$J/pulse, $\Delta t$ = 250 fs, $T$ = −5 °C, Movie S11). Each laser pulse generated impulses (shockwave, cavitation bubbles, etc.) as shown in Figure 4a−d, which caused the breaking, creation, and merging of bubbles. The temporal evolution of branch length corresponding to $L$ marked in Figure 5a is shown in Figure 5b. We found that the branch growth was transiently accelerated for the first ~300 $\mu$s after laser irradiation. Figure 5c shows the relationship between growth velocities of the tip of ice crystals immediately before and after a laser shot (slope $V_2$ and $V_1$ in Figure 5b, respectively). $V_1$ reached ~2.8 cm/s, which is much faster than that of as-grown ice crystals (~1.0 cm/s)[3]. Such growth promotion is probably due to the extraction of latent heat by water flow[20] generated by the laser-induced impulses. It is known that crystallization from melt-like ice crystallization is substantially influenced by latent heat.[34] The relationship in Figure 5c can be explained by the following hypothesis. A small $V_2$ means that the crystal generates a large latent heat, whose extraction produces a large $V_1$. In contrast, a large $V_2$ means that the crystals generate a small latent heat, resulting in a small $V_1$. Enhancement of heat transfer is well reported in ultrasound studies, which can also be explained by water flow.[35,36] Such crystal growth promotion by laser-induced impulses through focused irradiation into "liquid" is a different mechanism from that of our previous works where crystal growth was promoted via laser ablation of a "crystal"[37−40] and will offer a new approach for controlling crystal growth.

In this study, we improved spatiotemporal resolution for imaging of dynamics of ice crystallization including nucleation at the micrometer and microsecond scales. Such precise monitoring should be realized by the high spatiotemporal controllability of ice crystallization with ultrashort laser irradiation. First, an ultrashort laser can locally generate laser-induced impulses due to the generation of shockwaves and cavitation bubbles at the laser focus. Focused irradiation with ultrashort lasers in a transparent medium efficiently induces multiphoton absorption, which makes the excitation volume smaller than the diffraction limit.[41] In addition, we set the wavelength of the incident laser to ~800 nm because water is more transparent at 800 nm than at 1064 nm (absorption coefficient: 800 nm, 0.02 $cm^{-1}$; 1064 nm, 0.13 $cm^{-1}$).[32,42] We also used a lens with a higher numerical aperture (NA = 0.4 or 0.25) than that used in a study with a nanosecond laser (NA is calculated to be ~0.16).[18] We consider that the tightly focused laser pulse, for which water is optically transparent, also



https://doi.org/10.1021/acs.jpclett.3c00414
J. Phys. Chem. Lett. 2023, 14, 4394−4402

contributes to minimizing the excited volume. Such a smaller excited volume with an ultrashort laser can well localize laser-induced impulses near a focal spot, which improves the spatial controllability of ice crystal nucleation in this study compared to that in the study with the nanosecond laser.[18] In fact, the cavitation bubbles induced by a femtosecond and picosecond laser (radius: 60−330 $\mu$m, Figure S2) are smaller than those induced by a nanosecond laser (470−580 $\mu$m) by Lindinger et al.[18]

Second, an ultrashort laser can suppress the temperature elevation compared with a nanosecond laser. In the nanosecond pulse excitation process, heat generation by recurring electron excitation and relaxation results in significant temperature elevation at the laser focus.[22] On the other hand, in the ultrashort pulse excitation process, the increase in heat in molecules by rapid electron excitation and relaxation is preferentially converted into thermoelastic pressure that induces shock and stress waves.[22] The propagation of these waves suppresses temperature elevation at the laser focus, although it induces pressure depression. Lindinger et al. pointed out that temperature elevation due to laser irradiation retarded the detection of ice crystals,[18] which may degrade the temporal resolution of imaging for capturing crystallization dynamics. Therefore, we consider that such a well-localized laser-induced impulse with smaller heat effects with an ultrashort laser resulted in the precise spatiotemporal controllability of ice crystallization and thus realized the fine observation of crystallization dynamics in this study. It should also be noted that the imaging spatiotemporal resolution of ice crystallization in this study was also finer than that using other external stimuli, such as electric effects[43] or ultrasound,[44] as well as that of crystallization from liquid induced by other types of optical effects (e.g., photoelectric fields).[19,45,46]

Next, we discuss the mechanism of the laser-induced ice nucleation. As represented in Figure 4e, the high-speed imaging of laser-induced ice crystallization indicates that crystal nucleation takes place within ∼300 $\mu$s after the laser shot, implying that several phenomena, such as generation of shockwaves, cavitation bubbles, and long-lasting bubbles, play a crucial role for ice crystal nucleation. When an ultrafast laser pulse with the energy beyond ablation threshold is shot into water, in a submicroscond time scale, a shockwave is generated and propagates away from a laser focus with the velocity beyond that of sound in water (∼$10^3$ m/s). During the shockwave propagation, water in the region of few tens of micrometers from the focal spot experiences pressure of GPa to MPa.[33] Then a laser-induced cavitation bubble generates and shows repeated expansion and shrinkage within ∼10 $\mu$s after the laser shot. Afterward, the cavitation bubble finally collapses in tens of microseconds after a laser shot with generation of pressure waves and long-lasting bubbles that remain in the water for several seconds.

Past studies reported that transient high-pressure fluctuation with GPa order possibly triggers crystal nucleation of ice by instantaneously increasing the supercooling degree of water.[47−49] Under such high-pressure conditions, several tens of Kelvin of supercooling can be expected,[49] which may be sufficient for induction of homogeneous nucleation of ice. Lindinger et al. also concluded that shockwaves and pressure waves were the main factors of laser-induced ice crystal nucleation.[18] Such a shockwave can be more localized in the case of the focused irradiation with ultrashort laser pulses, which should improve the spatial controllability of crystal nucleation. In addition, there are also a number of studies insisting that cavitation bubbles also play a crucial role in ice crystal nucleation by generation of transient pressure wave,[48,49] enhancement of heterogeneous nucleation,[50] inducing streaming flows,[51] etc.[52] It was reported that laser-indued cavitation bubbles can also induce crystal nucleation of various materials from solution.[23,53,54] In fact, the correlation between nucleation probability of ice (Figure 3a) and the size of cavitation bubbles (Figure S2) strongly suggests a crucial role of laser-induced cavitation bubbles in ice crystal nucleation. Considering the above-mentioned factors, it is reasonable that ice crystal nucleation soon after laser irradiation (Figure 4b,c; red and green plots in Figure 4e) is probably attributed to the effect of shockwave and/or cavitation bubble generation. Then crystals shown in Figure 4d that were formed in later time scale, approximately 300 $\mu$s after laser irradiation, are precipitated with long-lasting bubbles that can serve sites for heterogeneous nucleation.[55] Interestingly, we also found that the laser irradiation into the neighborhood of pre-existing bubbles that were generated with a prior pulse could drastically enhance ice crystal nucleation (Figure S4). This result indicates that ice nucleation shown in Figure 1 and 2 was also attributed to the interaction between laser-induced impulses and long-lasting bubbles. Overall, the focused irradiation with ultrashort pulses into liquids can provide various impulses, which can promote ice crystal nucleation with fine spatiotemporal controllability (within ∼100 $\mu$m from the laser focus and ∼300 $\mu$s from laser irradiation) against laser-induced heat jump.

In summary, we realized the fine spatiotemporal control of ice crystallization via focused irradiation with ultrashort laser pulses. The pulse induced an impulse that generated shockwaves and a cavitation bubble localized near the laser focus. With the benefit of ice nucleation due to the well-localized impulse, when the observation spot was tuned on the laser focus, crystallization initiated near the laser focus was observed without blurring. We realized high-speed and high-resolution imaging. From observations detected at spatiotemporal resolutions of micrometers and microseconds, we confirmed the morphologies, growth rate, and crystallization dynamics of ice in various aqueous solutions (pure water, glucose, sucrose, antifreeze protein, and plant extract solution). A systematic screening of laser parameters (laser energy and pulse duration) revealed that an ultrashort laser pulse can trigger ice crystal nucleation even with a single laser pulse, which enables us to observe crystallization dynamics with a resolution of several microseconds (125000 fps). With a sequential pulse irradiation with a repetition rate of 1 kHz, we observed a stepwise crystal growth that followed each pulse irradiation. This phenomenon suggests that a jet flow with shock and stress wave propagation diffuses latent heat at the growth tip and resets the growth. Namely, the growth dynamics include growth rates with and without latent heating. We foresee that this laser method will contribute to the study of ice crystallization in various natural and biological phenomena and industrial processes.

## ■ ASSOCIATED CONTENT

### Supporting Information

The Supporting Information is available free of charge at https://pubs.acs.org/doi/10.1021/acs.jpclett.3c00414.



https://doi.org/10.1021/acs.jpclett.3c00414
J. Phys. Chem. Lett. 2023, 14, 4394−4402

Experimental protocols, dependence of laser energy on crystal nucleation probability in 10 ns pulses, dependence of laser energy and pulse duration on maximum radius of cavitation bubble, and optical setup for ice crystallization (PDF)

Movie S1: Macroscopic ice crystallization dynamics in water triggered by laser pulses ($E$ = 10 $\mu$J/pulse, $\Delta t$ = 250 fs, 20 Hz, $T \approx -5$ °C); images captured at frame rate of ∼240 fps (MP4)

Movie S2: Microscopic ice crystallization dynamics in water triggered by laser pulses ($E$ = 3 $\mu$J/pulse, $\Delta t$ = 150 fs, 20 Hz, $T$ = −5 °C); images captured at frame rate of 10000 fps (MP4)

Movie S3: Microscopic ice crystallization dynamics in glucose solution triggered by laser pulses ($E \approx 3$ $\mu$J/pulse, $\Delta t$ = 150 fs, 20 Hz, $T$ = −5.0 °C); images captured at frame rate of 10000 fps (MP4)

Movie S4: Microscopic ice crystallization dynamics in sucrose solution triggered by laser pulses ($E \approx 3$ $\mu$J/pulse, $\Delta t$ = 150 fs, 20 Hz, $T$ = −5.0 °C); images captured at frame rate of 10000 fps (MP4)

Movie S5: Microscopic ice crystallization dynamics in antifreeze protein (type III) solution triggered by laser pulses ($E \approx 3$ $\mu$J/pulse, $\Delta t$ = 150 fs, 1 kHz, $T$ = −5.0 °C); images captured at frame rate of 10000 fps (MP4)

Movie S6: Microscopic ice crystallization dynamics in extract solution from Secale cereale by laser pulses ($E \approx$ 3 $\mu$J/pulse, $\Delta t$ = 150 fs, 20 Hz, $T$ = −5.0 °C); images captured at frame rate of 10000 fps (MP4)

Movie S7: Microscopic ice crystallization dynamics in extract solution from *Arabidopsis thaliana* by laser pulses ($E \approx 3$ $\mu$J/pulse, $\Delta t$ = 150 fs, 20 Hz, $T$ = −5.0 °C); images captured at frame rate of 10000 fps (MP4)

Movie S8: Macroscopic ice crystallization dynamics in water triggered by a single laser pulse ($E$ = 240 $\mu$J/pulse, $\Delta t$ = 5 ps, $T \approx -10$ °C); images captured at frame rate of 240 fps (MP4)

Movie S9: High-speed imaging of ice crystallization dynamics in water triggered by a single laser pulse ($E$ = 240 $\mu$J/pulse, $\Delta t$ = 5 ps, $T \approx -10$ °C); images captured at frame rate of 125000 fps (MP4)

Movie S10: High-speed imaging of ice crystallization dynamics in water triggered by a single laser pulse ($E$ = 240 $\mu$J/pulse, $\Delta t$ = 5 ps, $T \approx -10$ °C); images captured at frame rate of 62500 fps (MP4)

Movie S11: Stepwise growth enhancement of ice crystals in water triggered by laser pulses ($E$ = 1.3 $\mu$J/pulse, $\Delta t$ = 250 fs, $T$ = −5 °C); images captured at frame rate of 50000 fps (MP4)

## AUTHOR INFORMATION


### Corresponding Authors

**Yoichiroh Hosokawa** − *Division of Materials Science, Graduate School of Science and Technology, Nara Institute of Science and Technology, Ikoma, Nara 630-0192, Japan*; Email: hosokawa@ms.naist.jp

**Hiroshi Y. Yoshikawa** − *Department of Applied Physics, Graduate School of Engineering, Osaka University, Suita, Osaka 565-0871, Japan*; orcid.org/0000-0003-0624-6039; Email: hiroshi@ap.eng.osaka-u.ac.jp

### Authors

**Hozumi Takahashi** − *Department of Applied Physics, Graduate School of Engineering, Osaka University, Suita, Osaka 565-0871, Japan*

**Tatsuya Kono** − *Division of Materials Science, Graduate School of Science and Technology, Nara Institute of Science and Technology, Ikoma, Nara 630-0192, Japan*

**Kosuke Sawada** − *Division of Materials Science, Graduate School of Science and Technology, Nara Institute of Science and Technology, Ikoma, Nara 630-0192, Japan*

**Satoru Kumano** − *Division of Materials Science, Graduate School of Science and Technology, Nara Institute of Science and Technology, Ikoma, Nara 630-0192, Japan*

**Yuka Tsuri** − *Division of Materials Science, Graduate School of Science and Technology, Nara Institute of Science and Technology, Ikoma, Nara 630-0192, Japan*

**Mihoko Maruyama** − *Division of Electrical, Electronics and Infocommunications Engineering, Graduate School of Engineering, Osaka University, Suita, Osaka 565-0871, Japan; Graduate School of Life and Environmental Science, Kyoto Prefectural University, Sakyo-ku, Kyoto 606-8522, Japan*; orcid.org/0000-0002-3453-8007

**Masashi Yoshimura** − *Institute of Laser Engineering (ILE), Osaka University, Suita, Osaka 565-0871, Japan*

**Daisuke Takahashi** − *United Graduate School of Agricultural Sciences, Iwate University, Morioka 020-8550, Japan; Division of Life Science, Graduate School of Science & Engineering, Saitama University, Saitama 338-8570, Japan*

**Yukio Kawamura** − *United Graduate School of Agricultural Sciences and Department of Plant-bioscience, Faculty of Agriculture, Iwate University, Morioka 020-8550, Japan*

**Matsuo Uemura** − *United Graduate School of Agricultural Sciences and Department of Plant-bioscience, Faculty of Agriculture, Iwate University, Morioka 020-8550, Japan*; orcid.org/0000-0003-0436-2976

**Seiichiro Nakabayashi** − *Department of Chemistry and Division of Strategic Research and Development, Graduate School of Science and Engineering, Saitama University, Saitama 338-8570, Japan*; orcid.org/0000-0001-7427-0407

**Yusuke Mori** − *Division of Electrical, Electronics and Infocommunications Engineering, Graduate School of Engineering, Osaka University, Suita, Osaka 565-0871, Japan*

Complete contact information is available at: https://pubs.acs.org/10.1021/acs.jpclett.3c00414


### Notes

The authors declare no competing financial interest.

## ACKNOWLEDGMENTS

The present work was partly supported by grants from the Japan Society for the Promotion of Science (JSPS) KAKENHI (Nos. 22H00302, 22H05423, and 20K21117 to H.Y.Y.); the Ministry of Education, Culture, Sports, Science and Technology (MEXT) KAKENHI on Innovative Areas (Nos. 22120010 and JP18H05493 to Y.H., and 22120003 to M.U. and Y.K.); Takeda Science Foundation (H.Y.Y.); Uehara Memorial Foundation (H.Y.Y.); Amada Foundation (H.Y.Y.); The Naito Foundation (H.Y.Y.); the joint research project of Institute of Laser Engineering, Osaka University (2022B2-034 to H.Y.Y.); and Japan Science and Technology Agency (JST),



https://doi.org/10.1021/acs.jpclett.3c00414
J. Phys. Chem. Lett. 2023, 14, 4394−4402

SPRING (No. JPMJSP2138 to H.T.). H.T. is thankful for the support by Grant-in-Aid for JSPS fellows (No. 22J21666). We also thank Dr. Gen Sazaki (Hokkaido University, Japan) for fruitful discussion about the mechanism of laser-induced crystallization.

## REFERENCES

(1) Nakaya, U. *Snow Crystals: Natural and Artificial*; Harvard University Press: Cambridge, MA, 1954.
(2) Libbrecht, K. G. The physics of snow crystals. *Rep. Prog. Phys.* **2005**, *68*, 855−895.
(3) Shibkov, A.; Golovin, Y. I.; Zheltov, M.; Korolev, A.; Leonov, A. Morphology diagram of nonequilibrium patterns of ice crystals growing in supercooled water. *Physica A* **2003**, *319*, 65−79.
(4) Leborgne, N.; Teulieres, C.; Travert, S.; Rols, M. P.; Teissie, J.; Boudet, A. M. Introduction of specific carbohydrates into Eucalyptus gunnii cells increases their freezing tolerance. *Eur. J. Biochem.* **1995**, *229*, 710−717.
(5) Yeh, Y.; Feeney, R. E. Antifreeze proteins: structures and mechanisms of function. *Chem. Rev.* **1996**, *96*, 601−618.
(6) Nada, H.; Furukawa, Y. Antifreeze proteins: computer simulation studies on the mechanism of ice growth inhibition. *Polym. J.* **2012**, *44*, 690−698.
(7) Kiani, H.; Sun, D.-W. Water crystallization and its importance to freezing of foods: A review. *Trends Food Sci. Technol.* **2011**, *22*, 407−426.
(8) Langer, J.; Sekerka, R.; Fujioka, T. Evidence for a universal law of dendritic growth rates. *J. Cryst. Growth* **1978**, *44*, 414−418.
(9) Harrison, K.; Hallett, J.; Burcham, T.; Feeney, R.; Kerr, W.; Yeh, Y. Ice growth in supercooled solutions of antifreeze glycoprotein. *Nature* **1987**, *328*, 241−243.
(10) Tirmizi, S. H.; Gill, W. N. Effect of natural convection on growth velocity and morphology of dendritic ice crystals. *J. Cryst. Growth* **1987**, *85*, 488−502.
(11) Tirmizi, S. H.; Gill, W. N. Experimental investigation of the dynamics of spontaneous pattern formation during dendritic ice crystal growth. *J. Cryst. Growth* **1989**, *96*, 277−292.
(12) Koo, K.-K.; Ananth, R.; Gill, W. N. Tip splitting in dendritic growth of ice crystals. *Phys. Rev. A* **1991**, *44*, 3782−3790.
(13) Stan, C. A.; Schneider, G. F.; Shevkoplyas, S. S.; Hashimoto, M.; Ibanescu, M.; Wiley, B. J.; Whitesides, G. M. A microfluidic apparatus for the study of ice nucleation in supercooled water drops. *Lab Chip* **2009**, *9*, 2293−2305.
(14) Gurganus, C.; Kostinski, A. B.; Shaw, R. A. Fast imaging of freezing drops: No preference for nucleation at the contact line. *J. Phys. Chem. Lett.* **2011**, *2*, 1449−1454.
(15) McCloskey, J. P.; Karlsson, J. O. Temporally resolved imaging of ice nucleation and growth in highly supercooled water. In *2012 38th Annual Northeast Bioengineering Conference (NEBEC)*, Philadelphia, PA, USA, March 16−18, 2012; IEEE; pp 195−196.
(16) Acharya, P. V.; Bahadur, V. Fundamental interfacial mechanisms underlying electrofreezing. *Adv. Colloid Interface Sci.* **2018**, *251*, 26−43.
(17) Nalesso, S.; Bussemaker, M. J.; Sear, R. P.; Hodnett, M.; Lee, J. A review on possible mechanisms of sonocrystallisation in solution. *Ultrason. Sonochem.* **2019**, *57*, 125−138.
(18) Lindinger, B.; Mettin, R.; Chow, R.; Lauterborn, W. Ice crystallization induced by optical breakdown. *Phys. Rev. Lett.* **2007**, *99*, No. 045701.
(19) Nevo, I.; Jahn, S.; Kretzschmar, N.; Levantino, M.; Feldman, Y.; Naftali, N.; Wulff, M.; Oron, D.; Leiserowitz, L. Evidence for laser-induced homogeneous oriented ice nucleation revealed via pulsed x-ray diffraction. *J. Chem. Phys.* **2020**, *153*, No. 024504.
(20) Vogel, A.; Busch, S.; Parlitz, U. Shock wave emission and cavitation bubble generation by picosecond and nanosecond optical breakdown in water. *J. Acoust. Soc. Am.* **1996**, *100*, 148−165.
(21) Vogel, A.; Linz, N.; Freidank, S.; Paltauf, G. Femtosecond-laser-induced nanocavitation in water: implications for optical breakdown threshold and cell surgery. *Phys. Rev. Lett.* **2008**, *100*, No. 038102.
(22) Hosokawa, Y. Applications of the femtosecond laser-induced impulse to cell research. *Jpn. J. Appl. Phys.* **2019**, *58*, 110102.
(23) Yoshikawa, H. Y.; Murai, R.; Adachi, H.; Sugiyama, S.; Maruyama, M.; Takahashi, Y.; Takano, K.; Matsumura, H.; Inoue, T.; Murakami, S.; et al. Laser ablation for protein crystal nucleation and seeding. *Chem. Soc. Rev.* **2014**, *43*, 2147−2158.
(24) Alexander, A. J.; Camp, P. J. Non-photochemical laser-induced nucleation. *J. Chem. Phys.* **2019**, *150*, No. 040901.
(25) Heisterkamp, A.; Ripken, T.; Mamom, T.; Drommer, W.; Welling, H.; Ertmer, W.; Lubatschowski, H. Nonlinear side effects of fs pulses inside corneal tissue during photodisruption. *Appl. Phys. B: Laser Opt.* **2002**, *74*, 419−425.
(26) Barber, E. R.; Kinney, N. L.; Alexander, A. J. Pulsed laser-induced nucleation of sodium chlorate at high energy densities. *Cryst. Growth Des.* **2019**, *19*, 7106−7111.
(27) Haynes, W. M. *CRC Handbook of Chemistry and Physics*; CRC Press: Boca Raton, FL, 2014.
(28) Vorontsov, D. A.; Sazaki, G.; Titaeva, E. K.; Kim, E. L.; Bayer-Giraldi, M.; Furukawa, Y. Growth of ice crystals in the presence of type III antifreeze protein. *Cryst. Growth Des.* **2018**, *18*, 2563−2571.
(29) Kono, T.; Hosokawa, Y. Science As Art. *Oyobuturi* **2015**, *84*, 101 [in Japanese].
(30) Petzold, G.; Aguilera, J. M. Ice morphology: fundamentals and technological applications in foods. *Food Biophys.* **2009**, *4*, 378−396.
(31) Takahashi, H.; Sugiyama, T.; Nakabayashi, S.; Yoshikawa, H. Y. Crystallization from glacial acetic acid melt via laser ablation. *Appl. Phys. Express* **2021**, *14*, No. 045503.
(32) Vogel, A.; Noack, J.; Nahen, K.; Theisen, D.; Busch, S.; Parlitz, U.; Hammer, D.; Noojin, G.; Rockwell, B.; Birngruber, R. Energy balance of optical breakdown in water at nanosecond to femtosecond time scales. *Appl. Phys. B: Laser Opt.* **1999**, *68*, 271−280.
(33) Noack, J.; Hammer, D. X.; Noojin, G. D.; Rockwell, B. A.; Vogel, A. Influence of pulse duration on mechanical effects after laser-induced breakdown in water. *J. Appl. Phys.* **1998**, *83*, 7488−7495.
(34) Kobayashi, R. Modeling and numerical simulations of dendritic crystal growth. *Physica D* **1993**, *63*, 410−423.
(35) Kiani, H.; Sun, D.-W.; Zhang, Z. The effect of ultrasound irradiation on the convective heat transfer rate during immersion cooling of a stationary sphere. *Ultrason. Sonochem.* **2012**, *19*, 1238−1245.
(36) Floros, J. D.; Liang, H. Acoustically assisted diffusion through membranes and biomaterials. *Food Technol.* **1994**, *48*, 79−84.
(37) Tominaga, Y.; Maruyama, M.; Yoshimura, M.; Koizumi, H.; Tachibana, M.; Sugiyama, S.; Adachi, H.; Tsukamoto, K.; Matsumura, H.; Takano, K.; et al. Promotion of protein crystal growth by actively switching crystal growth mode via femtosecond laser ablation. *Nat. Photonics* **2016**, *10*, 723−726.
(38) Suzuki, D.; Nakabayashi, S.; Yoshikawa, H. Y. Control of Organic Crystal Shape by Femtosecond Laser Ablation. *Cryst. Growth Des.* **2018**, *18*, 4829−4833.
(39) Wu, C. S.; Ikeyama, J.; Nakabayashi, S.; Sugiyama, T.; Yoshikawa, H. Y. Growth Promotion of Targeted Crystal Face by Nanoprocessing via Laser Ablation. *J. Phys. Chem. C* **2019**, *123*, 24919−24926.
(40) Takahashi, H.; Yamaji, M.; Ikeyama, J.; Nakajima, M.; Kitahara, H.; Tetsukawa, S.; Kobayashi, N.; Maruyama, M.; Sugiyama, T.; Okada, S.; et al. Growth Enhancement of Organic Nonlinear Optical Crystals by Femtosecond Laser Ablation. *J. Phys. Chem. C* **2021**, *125*, 8391−8397.
(41) Korte, F.; Serbin, J.; Koch, J.; Egbert, A.; Fallnich, C.; Ostendorf, A.; Chichkov, B. Towards nanostructuring with femtosecond laser pulses. *Appl. Phys. A: Mater. Sci. Process.* **2003**, *77*, 229−235.
(42) Hendrik, B.; Hakvoort, J. H. M.; Donze, M. Optical properties of pure water. *Proc.SPIE* **1994**, *2258*, 174−183.


https://doi.org/10.1021/acs.jpclett.3c00414
J. Phys. Chem. Lett. 2023, 14, 4394−4402

(43) Yang, F.; Shaw, R. A.; Gurganus, C. W.; Chong, S. K.; Yap, Y. K. Ice nucleation at the contact line triggered by transient electrowetting fields. *Appl. Phys. Lett.* **2015**, *107*, 264101.
(44) Chow, R.; Mettin, R.; Lindinger, B.; Kurz, T.; Lauterborn, W. The importance of acoustic cavitation in the sonocrystallisation of ice-high speed observations of a single acoustic bubble. In *IEEE Symposium on Ultrasonics, 2003*, Honolulu, HI, USA, October 5−8, 2003; IEEE; Vol. 2, pp 1447−1450.
(45) Duffus, C.; Camp, P. J.; Alexander, A. J. Spatial control of crystal nucleation in agarose gel. *J. Am. Chem. Soc.* **2009**, *131*, 11676−11677.
(46) Urquidi, O.; Brazard, J.; LeMessurier, N.; Simine, L.; Adachi, T. B. In situ optical spectroscopy of crystallization: One crystal nucleation at a time. *Proc. Natl. Acad. Sci. U.S.A.* **2022**, *119*, No. e2122990119.
(47) Dolan, D.; Gupta, Y. Nanosecond freezing of water under multiple shock wave compression: Optical transmission and imaging measurements. *J. Chem. Phys.* **2004**, *121*, 9050−9057.
(48) Hickling, R. Nucleation of freezing by cavity collapse and its relation to cavitation damage. *Nature* **1965**, *206*, 915−917.
(49) Hickling, R. Transient, high-pressure solidification associated with cavitation in water. *Phys. Rev. Lett.* **1994**, *73*, 2853.
(50) Kordylla, A.; Krawczyk, T.; Tumakaka, F.; Schembecker, G. Modeling ultrasound-induced nucleation during cooling crystallization. *Chem. Eng. Sci.* **2009**, *64*, 1635−1642.
(51) Zhang, X.; Inada, T.; Tezuka, A. Ultrasonic-induced nucleation of ice in water containing air bubbles. *Ultrason. Sonochem.* **2003**, *10*, 71−76.
(52) Chow, R. C.; Atkins, D.; Singleton, S.; Mettin, R.; Lindinger, B.; Kurz, T.; Lauterborn, W.; Povey, M.; Chivers, R. High-speed observations of the nucleation of ice by power ultrasound. In *Water Properties of Food, Pharmaceutical, and Biological Materials*; del Pilar Buera, M., Welti-Chanes, J., Lillford, P. J., Corti, H. R., Eds.; CRC Press, 2006; pp 613−622.
(53) Nakamura, K.; Hosokawa, Y.; Masuhara, H. Anthracene crystallization induced by single-shot femtosecond laser irradiation: Experimental evidence for the important role of bubbles. *Cryst. Growth Des.* **2007**, *7*, 885−889.
(54) Soare, A.; Dijkink, R.; Pascual, M. R.; Sun, C.; Cains, P. W.; Lohse, D.; Stankiewicz, A. I.; Kramer, H. J. Crystal nucleation by laser-induced cavitation. *Cryst. Growth Des.* **2011**, *11*, 2311−2316.
(55) Heneghan, A.; Haymet, A. Liquid-to-crystal heterogeneous nucleation: bubble accelerated nucleation of pure supercooled water. *Chem. Phys. Lett.* **2003**, *368*, 177−182.





https://doi.org/10.1021/acs.jpclett.3c00414
*J. Phys. Chem. Lett.* 2023, 14, 4394−4402